World Electric Vehicle Journal Vol. 3 - ISSN 2032-6653 - © 2009 AVERE

EVS24
Stavanger, Norway, May 13 - 16, 2009

Rolling Stability Control Based on Electronic Stability Program for In-wheel-motor Electric Vehicle

Kiyotaka Kawashima, Toshiyuki Uchida, Yoichi Hori
University of Tokyo, Tokyo, Japan, kawashima@horilab.iis.u-tokyo.ac.jp

Abstract

In this paper, a novel robust rolling stability control (RSC) based on electronic stability program (ESP) for electric vehicle (EV) is proposed. Since EVs are driven by electric motors, they have the following four remarkable advantages: (1) motor torque generation is quick and accurate; (2) motor torque can be estimated precisely; (3) a motor can be attached to each wheel; and (4) motor can output negative torque as a brake actuator. These advantages enable high performance three dimensional vehicle motion control with a distributed in-wheel-motor system. RSC is designed using two-degree-of-freedom control (2-DOF), which achieves tracking capability to reference value and disturbance suppression. Generally, RSC and YSC are incompatible. Therefore, ESP, which is composed of estimation system(S1) and integrated vehicle motion control system(S2) is proposed. A distribution ratio of RSC and YSC is defined based on rollover index (RI) which is calculated in S1 from rolling state information. The effectiveness of proposed methods are shown by simulation and experimental results.

Keywords:rolling stability control, electric vehicle, disturbance observer, two-degrees-of-freedom control, vehicle motion control, identification

Nomenclature

a_x, a_y:Longitudinal and lateral acceleration
a_{yd}:Lateral acceleration disturbance
a_{yth}:Critical lateral acceleration
c_f, c_r:Front and rear tire cornering stiffness
C_r:Combined roll damping coefficient
d, d_f, d_r:Tread at CG, front and rear axle
$F_{xfl}, F_{xfr}, F_{xrl}, F_{xrr}$:Tire longitudinal forces
$F_{yfl}, F_{yfr}, F_{yrl}, F_{yrr}$:Tire lateral forces
$F_{zfl}, F_{zfr}, F_{zrl}, F_{zrr}$:Tire normal forces
g:Gravity acceleration
h_c, h_{cr}:Hight of CG and distance from CG to roll center
I_r:Moment of inertia about roll axis (before wheel-lift-off)
I_{r2}:Moment of inertia about roll axis (after wheel-lift-off)
I_y:Moment of inertia about yaw axis
K_r:Combined roll stiffness coefficient
l, l_f, l_r:Wheelbase and distance from CG to front and rear axle
M, M_s, M_u,:Vehicle, sprung and unsprung mass
N:Yaw moment by differential torque
V, V_w:Vehicle and wheel speed
β, γ:Body slip angle and yaw rate
δ:Tire steering angle
$\phi, \dot{\phi}$:Roll angle and roll rate
$\phi_{th}, \dot{\phi}_{th}$:Threshold of roll angle and roll rate

1 Introduction

1.1 In-wheel-Motor Electric Vehicle's Advantages and Application to Vehicle Motion Control

Electric vehicles (EVs) with distributed in-wheel-motor systems attract global attention not only from the environmental point of view, but also from the vehicle motion control. In-wheel-motor EVs can realize high performance vehicle motion control by utilizing advantages of electric motors which internal combustion engines do not have. The EV has the following four remarkable advantages [1]:

- Motor torque response is 10-100 times faster than internal combustion engine's one. This property enables high performance adhesion control, skid prevention and slip control.
- Motor torque can be measured easily by observing motor current. This property can be used for road condition estimation.
- Since an electric motor is compact and inexpensive, it can be equipped in each wheel. This fea-

World Electric Vehicle Journal Vol. 3 - ISSN 2032-6653 - © 2009 AVERE

ture realizes high performance three dimensional vehicle motion control.

- There is no difference between acceleration and deceleration control. This actuator advantage enables high performance braking control.

Slip prevention control is proposed utilizing fast torque response [1]. Road condition and skid detection methods are developed utilizing the advantage that torque can be measured easily [1]. Yawing stability control, side slip angle estimation and control methods are also proposed by utilizing a distributed in-wheel-motor system [2] - [4].

1.2 Background and Purpose of the Research

The purpose of this paper is to propose integrated rolling and yawing stability control (RSC and YSC). Rollover stability is important for all classes of light-vehicles such as light trucks, vans, SUVs and especially, for EVs which have narrow tread and high CG because EV is suitable for relatively small vehicle and human height does not change. According to the data from NHTSA, ratio of rollover accidents of pick ups' and vans' crashes in 2002 was only 3% against whole accidents. However, nearly 33% of all deaths from passenger vehicle crashes are due to rollover accidents [5]. Therefore, RSC is very important not only for ride quality but also for safety.
The RSC system has been developed by several automotive makers and universities [6] [7]. Rollover detection systems, such as rollover index (RI) [8] and Time-to-rollover (TTR) [9] are proposed for mitigating critical rolling motion.
Every system controls braking force on each wheel independently and suppresses sudden increase of lateral acceleration or roll angle. However, since braking force is the average value by pulse width modulation control of brake pad, brake system cannot generate precise torque or positive torque. In the case of in-wheel-motor, both traction and braking force can be realized quickly and precisely.
In addition to actuator advantages, RSC is designed by utilizing two-degrees-of-freedom (2-DOF) control based on disturbance observer (DOB) [10]. For the vehicle motion control field, DOB is applied to vehicle yaw/pitch rate control [2] [3] and 2-DOF control is applied to the electric power steering control [11]. There are three reasons to utilize DOB: 1)disturbance suppression, 2)nominalize lateral vehicle model and 3)tracking capability to reference value. DOB loop that suppresses the effect of disturbance, is faster than outer loop that achieves tracking capability. Designing DOB for traction force is not applicable for ICEV, because engine torque is not accurately known and long time delay exists. Therefore, DOB is applicable only in case of EVs. The tracking capability and robustness for lateral acceleration disturbance against such as side blast are realized by the proposed method.
However, roll and yaw stabilities are incompatible. High rolling stability makes vehicle behavior under steer. On the other hand, high yawing stability to avoid vehicle side slip, vehicle roll stability is not guaranteed. In the next section, electronic stability program (ESP) on EV is introduced using RI based on vehicle geometry and dynamics model, which achieves integrated three dimensional vehicle motion control.

2 Electronic Stability Program for Electric Vehicle

2.1 Introduction of Electronic Stability Program

Fig. 1 shows concept of ESP for EV. ESP consists of two systems; vehicle/road state estimation system (S1) and integrated vehicle motion control system (S2). S1 integrates information from sensors (accelerometer, gyro, GPS, suspension stroke and steering angle sensors) and estimates unknown vehicle parameters (mass), vehicle state variables (yaw rate, lateral acceleration, roll angle, roll rate and normal forces on tires) and environmental state variables [7] [12].
According to the information from S1, S2 controls vehicle dynamics using RSC and YSC, pitching stability control (PSC) and anti-slip control (ASC). According to RI, which is calculated by S1, a proper stability control strategy (YSC, RSC or mixed) is determined.
RSC is based on DOB and nominal vehicle state is calculated by a controller. If there are errors between calculated and actual dynamics, it is compensated by differential torque.

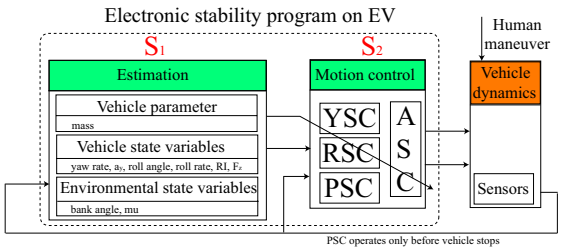

Figure 1: ESP based on DOB

2.2 A Scheme of Integrated Vehicle Motion Control

Lateral acceleration is composed of vehicle side slip, yaw rate and longitudinal speed.

$$a_y = (\dot{\beta} + \gamma)V \tag{1}$$

If constant vehicle speed is assumed and lateral acceleration is suppressed, yaw rate is also suppressed as long as differentiation of side slip is not controlled. This physical constraint makes RSC and YSC incompatible. Therefore, rollover detection is necessary for integrated control. In order to detect rollover, Yi proposed RI ($0 < RI < 1$) as a rollover detection [8]. When RI is high which means a vehicle is likely to roll over, the weight of RSC is set as high. On the other hand, RI is small, which means a vehicle is not likely to roll over, the weight of YSC is set as high.
Control algorithm is simple and given by following equation. Fig. 2 shows block diagram of three dimensional integrated vehicle motion control.

World Electric Vehicle Journal Vol. 3 - ISSN 2032-6653 - © 2009 AVERE

$$N^* = f(RI, N_{RSC}, N_{YSC}, N_{DOB}) = RI * N_{RSC} + (1 - RI) * N_{YSC} + N_{DOB} \quad (2)$$

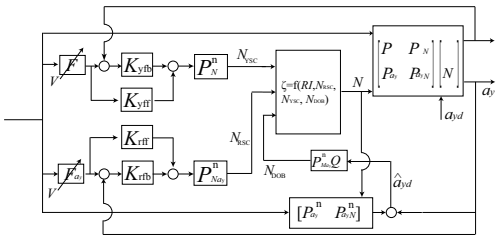

Figure 2: Block diagram of integrated vehicle motion control

3 Estimation System

S1 is composed of vehicle parameters, state variables and environmental state variables estimation system. In this section, vehicle state variable estimation system is mainly introduced. According to the estimated state variables, RI, a distribution ratio of RSC and YSC is determined.

3.1 Lateral Acceleration and Roll Angle Observer

Fig. 3 shows four wheel model and rolling model of electric vehicle.

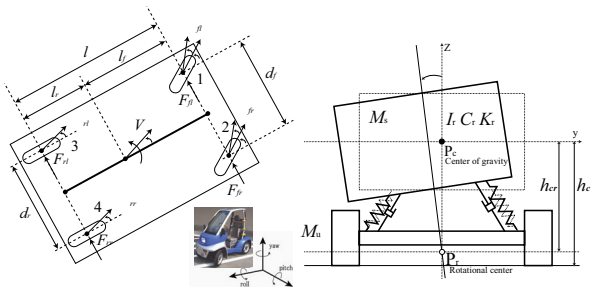

(a)Four wheel model and rotational direction

(b)Rolling model

Figure 3: Vehicle model

Vehicle motion is expressed as the following three linear equations.
Lateral motion:

$$MV(\dot{\beta} + \gamma) = F_{yfl} + F_{yfr} + F_{yrl} + F_{yrr} = -2c_f(\beta + \frac{l_f}{V}\gamma - \delta) - 2c_r(\beta - \frac{l_f}{V}\gamma) \quad (3)$$

Yawing motion:

$$I_y\dot{\gamma} = (F_{yfl} + F_{yrl})l_f - (F_{yfr} + F_{yrr})l_r = -2c_f(\beta + \frac{l_f}{V}\gamma - \delta)l_f + 2c_r(\beta - \frac{l_r}{V}\gamma)l_r + N \quad (4)$$

Rolling motion:

$$M_s h_{cr} a_y = I_r\ddot{\phi} + C_r\dot{\phi} + K_r\phi - M_s g h_{cr} sin\phi \quad (\phi < \phi_{wheel-lift-off}) \quad (5)$$

$$M_s h_{cr} a_y = I_{r2}\ddot{\phi} - M_s g h_{cr} sin\phi + M_s g\frac{d}{2}cos\phi \quad (\phi > \phi_{wheel-lift-off}) \quad (6)$$

Here, these motion equations need to be expressed as state equations to design observer. Observer gain matrix, however, becomes 2×4 matrix if whole equations are combined. To reduce redundancy of designing gain matrix, tire dynamics and rolling dynamics are separated. A matrix, A_{rt} connects two state equations.
From eq.(3) and eq.(4), state equation is expressed as,

$$\dot{\mathbf{x}}_t = A_t\mathbf{x}_t + B_t\mathbf{u}, \quad (7)$$
$$y_t = C_t\mathbf{x}_t + D_t\mathbf{u}. \quad (8)$$

It is noted that there is feedforward term in the transfer function from $\mathbf{u}$ to y_t. Therefore, to eliminate feedforward term and design stable observer, x_t vector is defined using differential torque and steering angle as the following equations, where,

$$\mathbf{x_t} = \begin{bmatrix} a_y - c_2\delta & \dot{a_y} - c_2\dot{\delta} - b_1 N - c_1\delta \end{bmatrix}^T,$$
$$y_t = a_y, \mathbf{u} = \begin{bmatrix} N & \delta \end{bmatrix}^T,$$

$$A_t = \begin{bmatrix} 0 & 1 \\ -a_0 & -a_1 \end{bmatrix},$$
$$B_t = \begin{bmatrix} b_1 & c_1 \\ a_1 b_1 + b_0 & a_1 c_1 + c_0 \end{bmatrix},$$
$$C_t = \begin{bmatrix} 1 & 0 \end{bmatrix}, D_t = \begin{bmatrix} 0 & c_2 \end{bmatrix}.$$

$$a_0 = \frac{4c_f c_r l^2}{MI_y V^2} - \frac{2(c_f l_f - c_r l_r)}{I_y},$$
$$a_1 = \frac{2M(c_f l_f^2 + c_r l_r^2) + 2I_y(c_f + c_r)}{MI_y V},$$
$$b_0 = \frac{2(c_f + c_r)}{MI_y}, b_1 = -\frac{2(c_f l_f - c_r l_r)}{MI_y V},$$
$$c_0' = \frac{4c_f c_r l}{MI_y}, c_1' = \frac{4c_f c_r l_r l}{MI_y V}, c_2 = \frac{2c_f}{N},$$
$$c_0 = c_0' - a_0 c_2, c_1 = c_1' - a_1 c_2$$

From eq.(7), state space equation is,

$$\dot{\mathbf{x}}_r = A_r\mathbf{x}_r + A_{rt}y_t, \quad (9)$$
$$y_r = C_r\mathbf{x_r}, \quad (10)$$

World Electric Vehicle Journal Vol. 3 - ISSN 2032-6653 - © 2009 AVERE

where, $\mathbf{x_r} = \begin{bmatrix} \phi & \dot{\phi} \end{bmatrix}^T, y_r = \dot{\phi},$

$$A_r = \begin{bmatrix} 0 & 1 \\ -\frac{K_r - M_s g h_{cr}}{I_r} & -\frac{C_r}{I_r} \end{bmatrix}, A_{rt} = \begin{bmatrix} 0 & 0 \\ \frac{M_s h_{cr}}{I_r} & 0 \end{bmatrix},$$

$$C_r = \begin{bmatrix} 0 & 1 \end{bmatrix}.$$

These parameters are based on the experiment vehicle "Capacitor-COMS1" developed in our research group. The method to evaluate the values of c_f, c_r are referred to the paper [13], and rolling parameters to the paper [10]
It should be noted that lateral acceleration dynamics expressed as eq.(8) is a linear time varying system depending on vehicle speed. The states are observable at various longitudinal speed except for a very low speed. In the following sections, for repeatability reason, experiment has been done under constant speed control. Observer gains are defined by pole assignment.

3.2 Rollover Index

RI is a dimensionless number which indicates a danger of vehicle rollover. RI is defined using the following three vehicle rolling state variables; 1)present state of roll angle and roll rate of the vehicle, 2)present lateral acceleration of the vehicle and 3)time-to-wheel lift. RI is expressed as eq. (11),

$$\begin{aligned} RI &= C_1\Big(\frac{|\phi|\dot{\phi}_{th} + |\dot{\phi}|\phi_{th}}{\phi_{th}\dot{\phi}_{th}}\Big) + C_2\Big(\frac{|a_y|}{a_{yc}}\Big), \\ &\quad +(1-C_1-C_2)\Big(\frac{|\phi|}{\sqrt{\phi^2+\dot{\phi}^2}}\Big), \text{ if } \phi(\dot{\phi} - k_1\phi) > 0, \\ RI &= 0, \quad \text{else if} \quad \phi(\dot{\phi} - k_1\phi) \le 0, \end{aligned} \tag{11}$$

where, C_1,C_2 and k_1 are positive constants ($0 < C_1, C_2 < 1$).
a_{yth} is defined by vehicle geometry. Fig. 4 shows equilibrium lateral acceleration in rollover of a suspended vehicle. It shows the relation between vehicle geometry such as h, d and K_r and vehicle states such as ϕ and a_y. From the static rollover analysis, critical lateral acceleration a_{yth} which induces rollover, is defined.
Phase plane analysis is conducted using a_{yth} and roll dynamics (eq. 7). Fig. 5 shows phase plane plot under several initial condition (ϕ, $\dot{\phi}$) at critical lateral acceleration. Consequently, ϕ_{th} and $\dot{\phi}_{th}$ are defined by the analysis.

4 Integrated Motion Control System

4.1 Rolling Stability Control Based on Two-Degrees-of-Freedom Control

In this section, RSC based on 2-DOF control which achieves tracking capability to reference value and disturbance suppression is introduced.
For RSC, lateral acceleration is selected as controlling parameter because roll angle information is relatively slow due to roll dynamics (about 100ms).

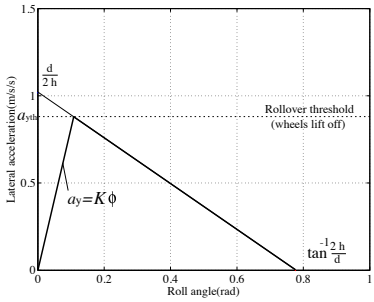

Figure 4: Equilibrium lateral acceleration in rollover of a suspended vehicle

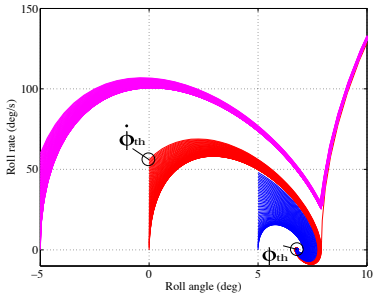

Figure 5: Phase plane plot of roll dynamics

4.1.1 Lateral acceleration disturbance observer

Based on fig. 6, transfer function from reference lateral acceleration u, δ and a_{yd} to a_y is expressed as the following equation. Roll moment is applied by differential torque N^* by right and left in-wheel-motors. Reference value of lateral acceleration is given by steering angle and vehicle speed.

$$\begin{aligned} a_y &= \frac{P_{a_yN}P^n_{Na_y}(K_{ff}+K_{fb})}{1+P_{a_yN}P^n_{Na_y}K_{fb}}u + \frac{P_{a_y\delta}}{1+P_{a_yN}P^n_{Na_y}K_{fb}}\delta \\ &\quad + \frac{1}{1+P_{a_yN}P^n_{Na_y}K_{fb}}a_{yd}. \end{aligned} \tag{12}$$

Tracking capability and disturbance suppression are two important performances in dynamics system control and can be controlled independently. On the other hand, one-degree-of-freedom (1-DOF) control such as PID controller loses important information at subtracting actual value from reference one. In the control, there is only one way to set feedback gain as high to improve disturbance suppression performance, however the gain makes the system unstable.
Hence 2-DOF control in terms of tracking capability and disturbance suppression is applied to RSC. Proposed lateral acceleration DOB estimates external disturbance to the system using information; V, δ, N and a_y. Fig. 6 shows the block diagram of lateral acceleration DOB.

World Electric Vehicle Journal Vol. 3 - ISSN 2032-6653 - © 2009 AVERE

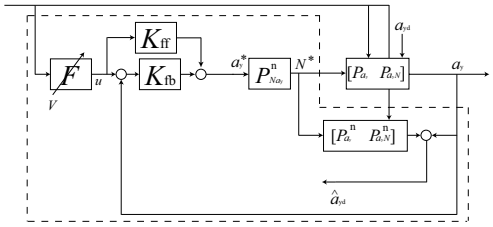

Figure 6: Block diagram of lateral acceleration DOB

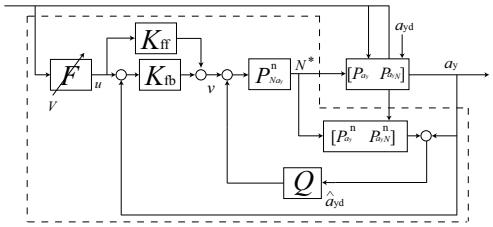

Figure 7: Block diagram of 2-DOF for RSC based on DOB

Estimated lateral acceleration disturbance $\hat{a}_{yd}$ and a_y are expressed as

$$\hat{a}_{yd} = a_y - P^n_{a_yN}N^* - P^n_{a_y\delta}\delta, \quad (13)$$

$$a_y = P_{a_yN}N^* + P_{a_y\delta}\delta + a_{yd}. \quad (14)$$

$$\hat{a}_{yd} = \frac{P^n_{Na_y}}{P_{Na_y}}\left(\left(\frac{P_{Na_y}}{P^n_{Na_y}} - 1\right)a_y + (P_{a_y\delta} - P^n_{a_y\delta})\delta + a_{yd}\right). \quad (15)$$

In eq. (15), the first and the second terms are modeling errors and the third term is lateral disturbance. If modeling error is small enough, a_{yth} is approximately equal to actual lateral acceleration disturbance.

4.1.2 Disturbance suppression and normalize of roll model

Fig. 7 shows the proposed 2-DOF control for RSC. Estimated lateral acceleration disturbance is fedback to lateral acceleration reference multiplied by filter Q.

$$a_y^* = v - Q\hat{a}_{yd}. \quad (16)$$

Filter Q is low pass filter and expressed as the following equation [14]. In this study, the cut-off frequency is set as 63 rad/s.

$$Q = \frac{1 + \sum_{k=1}^{N-r} a_k(\tau s)^k}{1 + \sum_{k=1}^{N} a_k(\tau s)^k}, \quad (17)$$

where r must be equal or greater than relative order of the transfer function of the nominal plant. Substituting eq. (16) to eq. (13), the following equation is defined.

$$a_y = v + P^n_{a_y\delta}\delta + (1 - Q)\hat{a_{yd}}. \quad (18)$$

Disturbance, which is lower than the cut-off frequency of Q and vehicle dynamics, is suppressed by DOB. In addition to the function of disturbance rejection, the plant is nearly equal to nominal model in lower frequency region than the cut-off frequency. Therefore the proposed RSC has the function of model following control.

4.2 Yawing Stability Control

As fig. 2 shows, YSC is yaw rate control. Yaw rate reference value is defined by steering angle and longitudinal vehicle speed. Transfer function from yaw rate reference and steering angle is expressed as the following equation.

$$\gamma = \frac{P_{\gamma N}P^n_{N\gamma}(K_{ff} + K_{fb})}{1 + P_{\gamma N}P^n_{N\gamma}K_{fb}}u + \frac{P_{\gamma\delta}}{1 + P_{\gamma N}P^n_{N\gamma}K_{fb}}\delta. \quad (19)$$

5 Simulation Results

Three dimensional vehicle motion simulations have been conducted with combination software of CarSim7.1.1 and MATLAB R2006b/Simulink.
At first, the effectiveness of RSC is verified. Lateral acceleration disturbance is generated by differential torque for repeatability reason of experiments. In the simulation, lateral blast is generated at straight and curve road driving, the proposed DOB suppresses the disturbance effectively.
To show the effectiveness of ESP, lateral acceleration response and trajectory at curving are compared. It is shown that lateral acceleration is unnecessarily suppressed only with RSC, however, tracking capability to yaw rate reference is achieved by ESP.

5.1 Effectiveness of RSC

5.1.1 Vehicle Stability under Crosswind Disturbance

Vehicle stability of RSC under crosswind disturbance is demonstrated. At first, the vehicle goes straight and a driver holds steering angle (holding steering wheel as 0 deg). Under 20 km/h vehicle speed control, crosswind is applied during 3-6 sec. Fig. 8 shows the simulation results.

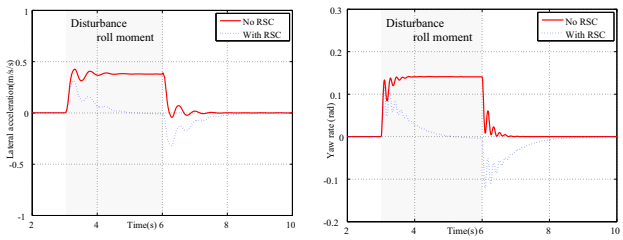

(a)Lateral acceleration (b)Yaw rate

Figure 8: Simulation result of RSC: Disturbance suppression at straight road drive

World Electric Vehicle Journal Vol. 3 - ISSN 2032-6653 - © 2009 AVERE

When proposed RSC is activated, the proposed lateral acceleration DOB detects the lateral acceleration disturbance and suppresses it.
Then, disturbance is applied at curve road driving. Under 20km/h constant speed control as well, 180 deg step steering is applied with roll moment disturbance during 3-6 sec. Fig. 9 shows decrease of lateral acceleration since disturbance is rejected perfectly by differential torque with RSC. The robustness of RSC is verified with simulation results.

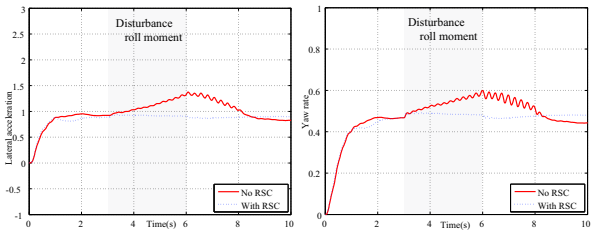

(a)Lateral acceleration (b)Yaw rate

Figure 9: Simulation result of RSC: Disturbance suppression at curving

5.1.2 Tracking capability to reference value

In this section, tracking capability of RSC to reference value is verified with simulation results. Under 20km/h vehicle speed control, 180 deg sinusoidal steering is applied and reference value of lateral acceleration is 80% of nominal value. Fig. 10 shows that lateral acceleration follows reference value with RSC.

5.2 Effectiveness of ESP

Rollover experiment can not be achieved because of safety reason. Under 20km/h constant speed control, 240 deg step steering is applied. From fig. 16, with only RSC case, even though the danger of rollover is not so high, lateral acceleration is strongly suppressed and trajectory of the vehicle is far off the road. On the other hand, with ESP case, the rise of lateral acceleration is recovered and steady state yaw rate is controlled so that it becomes close to no control case.

6 Experimental Results

6.1 Experimental setup

A novel one seater micro EV named "Capacitor COMS1" is developed for vehicle motion control experiments. The vehicle equips two in-wheel motors in the rear tires, a steering sensor, an acceleration sensor and gyro sensors to detect roll and yaw motion. An upper micro controller collects sensor information with A/D converters, calculates reference torques and outputs to the inverter with DA converter. In this system, sampling time is 1 (msec).
Fig. 12 shows the vehicle control system and TABLE I shows the specifications of the experimental vehicle.

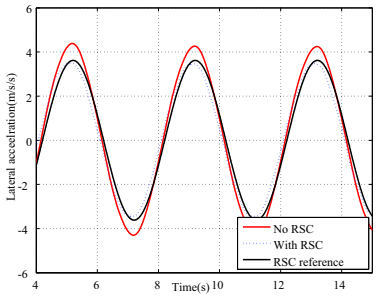

Figure 10: Simulation result of RSC: tracking capability to reference

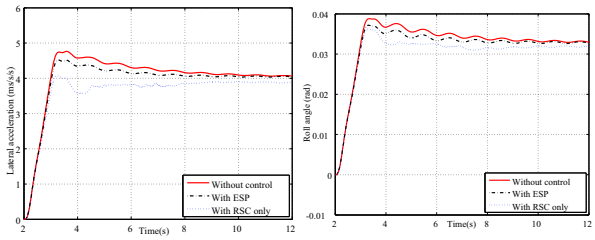

(a)Lateral acceleration (b)Roll angle

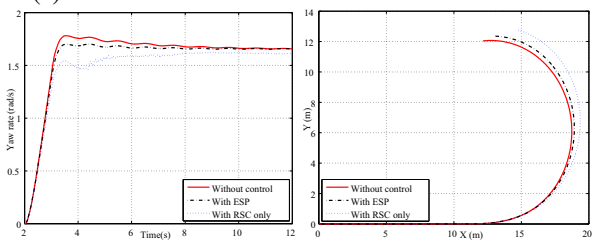

(c)Yaw rate (d)Trajectory

Figure 11: Simulation result of ESP: Step steering maneuver

At first, disturbance suppression performance and tracking capability to reference value are verified with experimental results. Then, effectiveness of ESP is demonstrated. In the experiment, since vehicle rollover experiment is not possible due to safety reason, step response of lateral acceleration and yaw rate are evaluated.

6.2 Effectiveness of RSC

6.2.1 Vehicle Stability under Crosswind Disturbance

For repeatability reason, roll moment disturbance is generated by differential torque. Under 20 km/h constant speed control, roll moment disturbance is applied from 1 sec. The disturbance is detected by DOB and compensated by differential torque of right and left in-wheel motors. Here, the cut-off frequency of the low pass filter is 63 rad/s.
Fig. 13 shows disturbance suppression during straight road driving. Step disturbance roll moment (equivalent

World Electric Vehicle Journal Vol. 3 - ISSN 2032-6653 - © 2009 AVERE

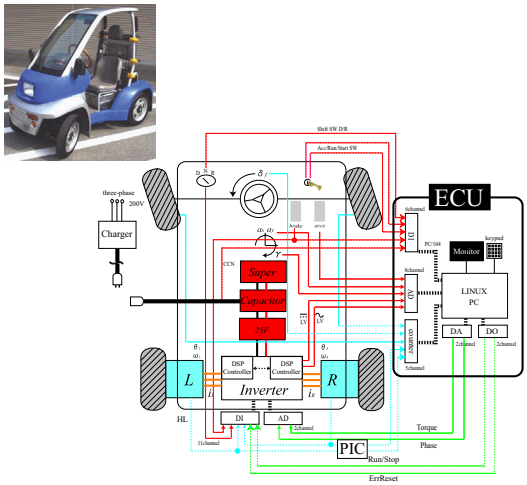

Figure 12: Control system of experimental vehicle

Table 1: Drive train specification of experimental vehicle

Motor	
Category	IPMSM
Phase/Pole	3/12
Rating power/Max	0.29kW/2kW
Max torque	100Nm
Max velocity	50km/h
Inverter	
Switching Hardware	MOS FET
Control method	PWM vector control

to $0.5m/s^2 * h_cr$) is applied around 1 sec. In the case without any control and only with FB control of RSC, lateral acceleration is not eliminated and vehicle trajectory is shifted in a wide range. On the other hand, in the case with DOB, disturbance is suppressed and vehicle trajectory is maintained.
Fig. 14 shows the experimental results of disturbance suppression at curve road driving. Under 20 km/h constant speed control, 240 deg steering is applied and disturbance is applied at around 2.5 sec. In this case, data is normalized by maximum lateral acceleration. In the case with RSC DOB, whole effect of disturbance is suppressed as no disturbance case. In the case without RSC, lateral acceleration decreases about 25% and vehicle behavior becomes unstable.

6.2.2 Tracking capability to reference value

In the previous section, since it was assured that the inner DOB loop is designed properly, tracking capability to reference value is verified with experimental results. 180 deg sinusoidal steering is applied and reference lateral acceleration is 80% of nominal value. The outer loop is designed with pole root loci method. Fig. 15

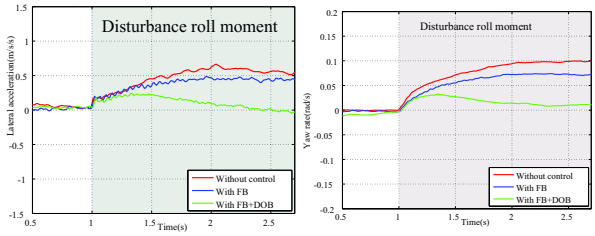

(a)Lateral acceleration (b)Yaw rate

Figure 13: Experimental result of RSC: Disturbance suppression at straight road drive

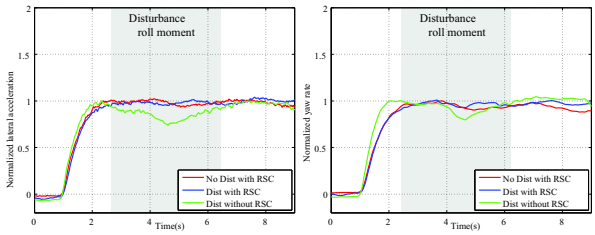

(a)Lateral acceleration (b)Yaw rate

Figure 14: Experimental result of RSC: Disturbance suppression at curve road driving

shows that in the case with RSC, tracking capability to reference value is achieved.

6.3 Effectiveness of ESP

Effectiveness of ESP is demonstrated by experiments. For safety reason, rollover experiment is impossible. Therefore, experimental condition is the same as 5.2. Under 20km/h constant speed control, 180 deg step steering is applied.
Fig. 16 shows that in the case with only RSC, lateral acceleration and yaw rate are strongly suppressed. On the other hand, in the case with ESP, yaw rate is recovered close to reference value. In addition, the rise of lateral acceleration is also recovered and stable cornering is achieved with ESP.

7 Conclusion

In this paper, a novel RSC based on ESP utilizing differential torque of in-wheel-motor EV is proposed. Effectiveness of novel RSC designed by 2-DOF control is verified with simulation and experimental results. Then incompatibility of RSC and YSC is described and ESP is proposed to solve the problem utilizing RI which is calculated using estimated value of estimation system of ESP. Experimental results validates the proposed ESP.

Acknowledgments

The author and the work are supported by Japan Society for the Promotion of Science.

World Electric Vehicle Journal Vol. 3 - ISSN 2032-6653 - © 2009 AVERE

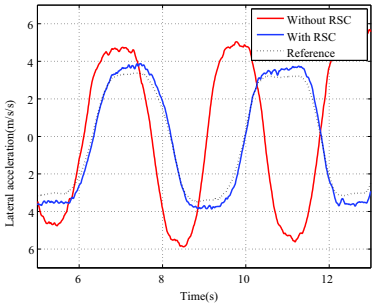

Figure 15: Experimental result of RSC: tracking capability to reference

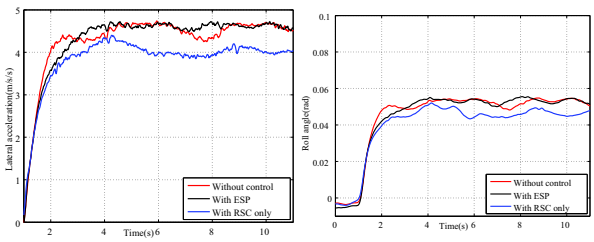

(a)Lateral acceleration

(b)Roll angle

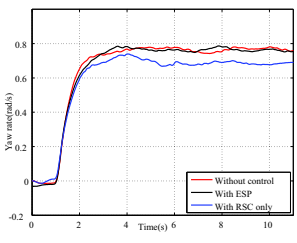

(c)Yaw rate

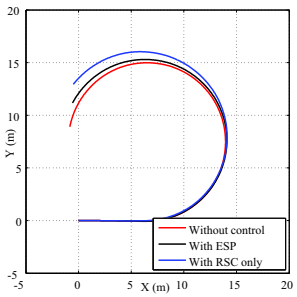

(d)Trajectory

Figure 16: Experimental result of ESP: Step steering maneuver

References

[1] Yoichi Hori, "Future Vehicle driven by Electricity and Control-Research on Four Wheel Motored UOT Electric March II", IEEE Transaction on Industrial Electronics, Vol.51, No.5, pp.954-962, 2004.10

[2] Hiroshi Fujimoto, Akio Tsumasaka, Toshihiko Noguchi, "Vehicle Stability Control of Small Electric Vehicle on Snowy Road", JSAE Review of Automotive Engineers, Vol. 27, No. 2, pp. 279-286, 2006.04

[3] Shinsuke Satou, Hiroshi Fujimoto, "Proposal of Pitching Control for Electric Vehicle with In-Wheel Motor", IIC-07-81 IEE Japan, pp.65-70, 2007.03 (in Japanese).

[4] Peng He, Yoichi Hori, "Improvement of EV Maneuverability and Safety by Dynamic Force Distribution with Disturbance Observer", WEVA-Journal, Vol.1, pp.258-263, 2007.05

[5] National highway traffic safety administration, Safercar program, http://www.nhtsa.gov/

[6] E. K. Liebemann, "Safety and Performance Enhancement: The Bosch Electronic Stability Control(ESP)", SAE Technical Paper Series, 2004-21-0060, 2004.10

[7] Hongtei E. Tseng, et al, "Estimation of land vehicle roll and pitch angles", Vehicle System Dynamics, Vol.45, No.5, pp.433-443, 2007.05

[8] Kyongsu Yi, et al, "Unified Chassis Control for Rollover Prevention, Maneuverability and Lateral Stability", AVEC2008, pp.708-713, 2008.10

[9] Bo-Chiuan Chen, Huei Peng,"Differential-Braking-Based Rollover Prevention for Sport Utility Vehicles with Human-in-the-loop Evaluations", Vehicle System Dynamics, Vol.36, No.4-5, pp359-389, 2001.

[10] Kiyotaka Kawashima, Toshiyuki Uchida, Yoichi Hori, "Rolling Stability Control of In-wheel Electric Vehicle Based on Two-Degree-of-Freedom Control", The 10th International Workshop on Advanced Motion Control, pp. 751-756, Trento Italy, 2008.03

[11] Bilin Aksun Guvenc, Tilman Bunte, Dirk Odenthal and Levent Guvenc, "Robust Two Degree-of-Freedom Vehicle Steering Controller Design", IEEE Transaction on Control Systems Technology, Vol. 12, No. 4, pp.627-636, 2004.07

[12] A. Hac, et. al, "Detection of Vehicle Rollover", SAE Technical Paper Series, 2004-01-1757, SAE World Congress, 2004.

[13] N. Takahashi, et. al, "Consideration on Yaw Rate Control for Electric Vehicle Based on Cornering Stiffness and Body Slip Angle Estimation", IEE Japan, IIC-06-04, pp.17-22, 2006

[14] Takaji Umeno, Yoichi Hori, "Robust Speed Control of DC Servomotors Using Modern Two Degrees-of-Freedom Controller Design", IEEE Transaction Industrial Electronics, Vol.38, No. 5, pp.363-368, 1991.10

Authors

He received B.C. and M.S. degrees in E.E. department, the University of Tokyo in 2004 and 2006, and proceeded to Ph.D. course, the University of Tokyo. He is now researching the motion control of electric vehicle.

He is working as a engineering official in E.E. department, the University of Tokyo

He received Ph.D degree in E.E. from the UT in 1983 and became a Professor in 2000. IEEE Fellow. He is now an AdCom member of IEEE-IES. He is the President of IEE-Japan IAS in 08'-09'. His research fields are control theory and its industrial application to EV, mechatronics, robotics, etc.